Extension of On-Surface Radiation Condition Theory to Scattering by Two-Dimensional Homogeneous Dielectric Objects

STEPHEN ARENDT, STUDENT MEMBER, IEEE, KORADA R. UMASHANKAR, SENIOR MEMBER, IEEE, ALLEN TAFLOVE, FELLOW, IEEE AND GREGORY A. KRIEGSMANN

***Abstract*—The recent new analytical formulation of electromagnetic wave scattering by perfectly conducting two-dimensional objects using the on-surface radiation boundary condition approach is conveniently extended to the case of two-dimensional homogeneous convex dielectric objects. The existing classical solution for the scattering and penetration analysis of dielectric objects is based upon coupled field formulation with the external and internal fields directly coupled together through the electromagnetic surface boundary conditions. It is shown here that a substantial simplification in the analysis can be obtained by applying the out-going radiation boundary condition on the surface of the convex homogeneous dielectric object. This analysis procedure decouples the fields in the two regions to yield explicitly a differential equation relationship between the external incident field excitation and the corresponding field distribution in the interior of dielectric object. The interior fields can be obtained by solving the differential equation using either an analytical approach or a suitable numerical method. Two dimensional scattering examples along with validations are reported showing the near surface field distributions for a homogeneous circular dielectric cylinder and an elliptic dielectric cylinder each with transverse magnetic plane wave excitation. The resulting surface currents are compared with good agreement to those obtained from the integral equation solution.**

I. Introduction

Recently a novel analytical technique based on the on-surface radiation condition (OSRC) theory [1] was introduced for modeling high-frequency electromagnetic wave scattering. For two-dimensional analysis of electromagnetic scattering by convex conducting objects, the OSRC approach has demonstrated substantial simplification of the usual integral equation for the induced surface currents through the application of a radiation boundary operator [2], [3] directly on the object surface. This method has been shown to give reasonable results for two-dimensional perfectly conducting objects having either transverse magnetic (TM) or transverse electric (TE) plane wave excitation [1] and also has been applied to various reactively loaded acoustic scattering problems [4]. The main purpose of this paper is to demonstrate further an extension and application of this novel OSRC analytical technique to the analysis of electromagnetic scattering and penetration by homogeneous convex dielectric objects.

Over the past several years, there has been substantial investigation in the development of expansions for local radiation boundary conditions of higher order than the Sommerfeld condition [5], [6]. The goal has been to achieve nearly reflection-free truncations of space grids used to model wave interactions with structures via direct finite-difference [7], [8] or finite-element simulations of the governing partial differential field or wave equations. The boundary operators, containing mixes of both space and time partial derivatives, principally exploit the asymptotic behavior of the scattered field in either cylindrical or spherical coordinate systems. While the radiation boundary operators have been successfully applied to the scattered field away from the specific scatterer of interest, the OSRC concept was prompted by the observation that the outer boundaries of finite-difference time-domain space grids [7] employing the second-order radiation boundary operator, could be brought very close to a scatterer without adversely affecting the far-field results. In a limit, if the radiation boundary condition is applied directly on a two-dimensional conducting scatterer surface, the original integral equation for the scattered field can be reduced to merely a line integral of known fields around the surface for the TM case, or an ordinary differential equation to be solved around the surface for the TE case, whereby analytical expressions for the induced surface current distribution can be obtained [1]. Interestingly enough, elaborate finite-difference numerical simulation schemes are no longer required which seems to depend on the accuracy needed. In order to extend the general applicability of the OSRC technique to the case of scattering and penetration involving re-entrant and other related cavity type interaction problems, a detailed study is reported in this paper concerning the electromagnetic scattering and interaction analysis of homogeneous convex dielectric objects. In fact, the formulation is applicable in the low frequency, resonant frequency, and also high frequency regimes. Specifically for the case of high frequency regimes

Manuscript received August 19, 1988; revised March 9, 1990. This work was supported in part by the Office of Naval Research under grant N00014-88-K-0475 to Northwestern University and the University of Illinois at Chicago.

S. Arendt was with the Department of Electrical Engineering and Computer Science, University of Illinois, Chicago, IL. He is now with the Department of Physics, University of Chicago, Chicago, IL 60637.

K. R. Umashankar is with the Department of Electrical Engineering and Computer Science, University of Illinois at Chicago, Chicago, IL 60680.

A. Taflove is with the Department of Electrical Engineering and Computer Science, Northwestern University, Evanston, IL 60208.

G. A. Kriegsmann is with the Department of Engineering Sciences and Applied Mathematics, Northwestern University, Evanston, IL 60208.

IEEE Log Number 9037626.

[4], an asymptotic expansion in terms of the wavenumber k can also be used in the derivation of the near and far scattered fields.

For the analysis of homogeneous dielectric objects [9], use of the dielectric boundary conditions in the OSRC differential equation yields a relation between the electric field and its normal derivative on the surface of the scatterer. As the OSRC equation is only valid over the boundary surface, one needs an additional relation between the electric field and its normal derivative on the scatterer contour to completely solve the problem. In this study, a functional form for the interior field distribution is specified, immediately providing the required additional relation through differentiation. Specifically, the interior electric field is represented by a modal expansion with unknown coefficients. For the case of general dielectric scatterer application, the functional form of differential equation can be analyzed based on an appropriate numerical method. For a circular dielectric cylinder, a direct substitution of this modal expansion into the OSRC equation followed by an enforcement of the orthogonality of the angular eigenfunctions gives a solution for the unknown coefficients. However, for a general dielectric cylinder, such a procedure is not applicable because a modal series defined in an arbitrary dielectric object is not guaranteed convergence at points everywhere on the scatterer contour, so that the boundary conditions cannot be applied to this expansion. To surmount this difficulty, an analytic continuation method is used [10], [11]. In this scheme, the interior field modal expansions are analytically continued throughout the scatterer interior in order to obtain series expansions which are valid on the contour of the dielectric scatterer. Once this is done, the OSRC differential equation can be used to apply the boundary conditions, yielding a matrix equation for the unknown expansion coefficients.

In the following, the application of the OSRC method to the case of homogeneous dielectric objects is outlined briefly beginning with the general dielectric OSRC equation and the solution for a homogeneous circular dielectric cylinder. A brief outline of the analytical continuation formulation, which is required only inside the scatterer, is then presented and applied to the case of a homogeneous dielectric elliptic cylinder. Numerical results for the surface electric and magnetic current distributions are presented for both the dielectric circular and elliptic cylinders having TM plane wave excitation. The TE excitation case is not reported here since it forms a trivial dual case. For the canonical dielectric case studies reported, good validations have been obtained based on the regular eigenfunction solution and the combined field coupled integral equation numerical solution [8], [12].

II. General Formulation

Let us consider a two-dimensional, convex, homogeneous dielectric scatterer excited normally by a TM polarized plane wave as shown in Fig. 1. The dielectric scatterer is assumed to be uniform in the z-coordinate direction. The cross section of the arbitrary convex cylinder is contained in region 2 and is bounded by a contour C. Outside region 2 is region 1 representing an isotropic free space medium. Referring to

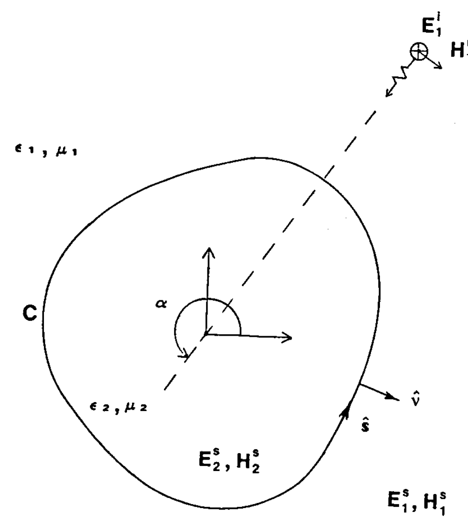

Fig. 1. Two-dimensional homogeneous dielectric scatterer.

Fig. 1, let

- ϵ_1, μ_1 permittivity and permeability of the free space region;
- ϵ_2, μ_2 permittivity and permeability of the dielectric material scatterer;
- $(\overline{\mathbf{E}}_1^s, \overline{\mathbf{H}}_1^s)$ electric and magnetic scattered fields in region 1;
- $(\overline{\mathbf{E}}_2^s, \overline{\mathbf{H}}_2^s)$ electric and magnetic scattered fields in region 2;
- $(\overline{\mathbf{E}}_1^i, \overline{\mathbf{H}}_1^i)$ electric and magnetic incident fields in region 1.

In the classical approach, the expressions for the scattered fields in regions 1 and 2 are obtained in terms of the surface electric and magnetic fields or in terms of the corresponding equivalent magnetic and electric currents on the contour C, by invoking the electromagnetic equivalence principle [8]. In the application of OSRC method for the electromagnetic scattering by the dielectric object, a higher order radiation boundary condition is enforced on the contour C of the convex scatterer itself. According to this approach, for the case of a TM excited two-dimensional smooth convex cylinder, the z-component of the scattered electric field in region 1 should satisfy the following radiation boundary condition [1]:

$$B_2 E_1^s \approx O(R^{-2m-1/2}) \tag{1a}$$

$$B_2 = \frac{\partial}{\partial \nu} + \frac{\xi}{2} + jk - \frac{1}{2(\xi + jk)}\left(\frac{\partial^2}{\partial s^2} + \frac{\xi^2}{4}\right) \tag{1b}$$

$$k = \omega[\mu_1 \epsilon_1]^{1/2} \tag{1c}$$

where R is the radius of large circle, k is the propagation factor in the free space region, ω is the frequency, $\partial/\partial\nu$ is the normal derivative, ξ and s are the curvature and arc length, respectively, along the contour C. Further, across the boundary contour C of the homogeneous dielectric cylinder, the z component of the electric fields and the transverse component of the magnetic fields are continuous, yielding the regular surface boundary conditions

$$E_1^s + E_1^i = E_2^s \tag{2a}$$

$$\hat{\mathbf{s}} \cdot (\overline{\mathbf{H}}_1^s + \overline{\mathbf{H}}_1^i) = \hat{s} \cdot \overline{\mathbf{H}}_2^s \tag{2b}$$

where $\hat{s}$ is a tangential vector to the contour C, and in terms of normal derivatives the expression (2b) takes the form

$$\frac{1}{\mu_1}\left(\frac{\partial E_1^i}{\partial \nu} + \frac{\partial E_1^s}{\partial \nu}\right) = \frac{1}{\mu_2}\frac{\partial E_2^s}{\partial \nu}. \tag{2c}$$

On substituting the boundary conditions (2a) and (2c) into the OSRC boundary operator (1),

$$\frac{\mu_1}{\mu_2}\frac{\partial E_2^s}{\partial \nu} + AE_2^s + B\frac{\partial^2 E_2^s}{\partial s^2} = \frac{\partial E_1^i}{\partial \nu} + AE_1^i + B\frac{\partial^2 E_1^i}{\partial s^2} \tag{3a}$$

where the coefficients A and B are given by

$$A = jk + \frac{\xi}{2} + \frac{j\xi^2}{8(k - j\xi)} \tag{3b}$$

$$B = \frac{j}{2(k - j\xi)}. \tag{3c}$$

The right-hand side of (3a) is simply equal to $B_2 E_1^i$, and, being a function of the incident field only, is completely known. For convenience, a second operator B_2^+ is introduced to represent the operation on E_2^s in the left side of (3a). This operator differs from the B_2 operator only in the permeability ratio multiplying the normal derivative. For the case of lossy materials, the permittivity and permeability parameters of the dielectric scatterer are redefined in terms of their effective values to take into account the conductivity parameter. It is known that the total electric field evaluated on the contour C is proportional to the equivalent magnetic surface current on C, and that the normal derivative of the electric field on C is proportional to the equivalent electric surface current on C. Thus, (3a) provides a relation between the equivalent electric and magnetic currents on the surface of the dielectric scatterer. Since (3a) is a relation between two unknowns, it alone is not enough to solve the scattering problem; an additional relation between the total electric field and its normal derivative on C is also necessary. If a functional form is assumed for the interior scattered electric field, the second required relation is immediately provided through differentiation. In the following section, the interior electric field of a circular cylinder will be represented by an eigenfunction expansion having unknown coefficients. This single expansion, when substituted into the relationship (3a), is enough to yield the unknown scattering coefficients. Once the electric field is known along the contour C, the corresponding scattered magnetic field along the contour C can be obtained by taking the normal derivative of the scattered electric field.

III. Scattering by a Dielectric Circular Cylinder

Consider the case of homogeneous dielectric circular cylinder of radius a illuminated by a TM polarized normally incident plane wave. In the regular dielectric scatterer analysis, one uses the electric and magnetic field boundary conditions (2a) and (2b) along with modal expansions for the interior and exterior scattered fields. However, in the OSRC analysis, one needs only an interior field modal expansion, and the expression (3a) which serves as a boundary condition for the interior field. For the case of circular cylindrical geometry, substituting $\nu = r$ and $s = r\phi$, (3a) takes the form

$$\frac{\mu_1}{\mu_2}\frac{\partial E_2^s}{\partial r} + AE_2^s + \frac{B}{r^2}\frac{\partial^2 E_2^s}{\partial \phi^2} = \frac{\partial E_1^i}{\partial r} + AE_1^i + \frac{B}{r^2}\frac{\partial^2 E_1^i}{\partial \phi^2} \tag{4a}$$

and the coefficients A and B are given by

$$A = jk + \frac{1}{2r} + \frac{j}{8r^2(k - j/r)} \tag{4b}$$

$$B = \frac{j}{2(k - j/r)}. \tag{4c}$$

A TM polarized normally incident plane wave having unit amplitude and propagating in the x direction can be written in terms of an infinite sum over cylindrical modes, and is given by

$$E_1^i(r, \phi) = e^{-jkx} = \sum_{m=-\infty}^{\infty} j^{-m} J_m(kr) e^{jm\phi}. \tag{5a}$$

For the dielectric region the interior scattered field can be similarly written as

$$E_2^s(r, \phi) = \sum_{m=-\infty}^{\infty} P_m J_m(k_2 r) e^{jm\phi} \tag{5b}$$

$$k_2 = \omega[\mu_2 \epsilon_2]^{1/2} \tag{5c}$$

where J_m is the Bessel function of first kind and of order m, P_m are the unknown scattering modal coefficients for the interior fields, and k_2 is the propagation constant for the dielectric region. By substituting the modal expansions (5a) and (5b) into the OSRC relationship (4a) and by invoking the orthogonality properties with respect to the angular variable ϕ on both sides of the expression, the various modal coefficients P_m can be determined

$$P_m = \frac{j^{-m}\left[kJ_m'(ka) - \left\{\frac{Bm^2}{a^2} - A\right\}J_m(ka)\right]}{\left[\frac{\mu_1}{\mu_2}k_2 J_m'(k_2 a) - \left\{\frac{Bm^2}{a^2} - A\right\}J_m(k_2 a)\right]}. \tag{6}$$

In fact, using the electric field boundary condition, expression (2a), the modal coefficients for the exterior fields can also be determined, if required. Similarly, the transverse magnetic field can be obtained by taking the normal derivative of the electric field. In fact, the electric and the magnetic fields along the contour C can be converted into the corre-

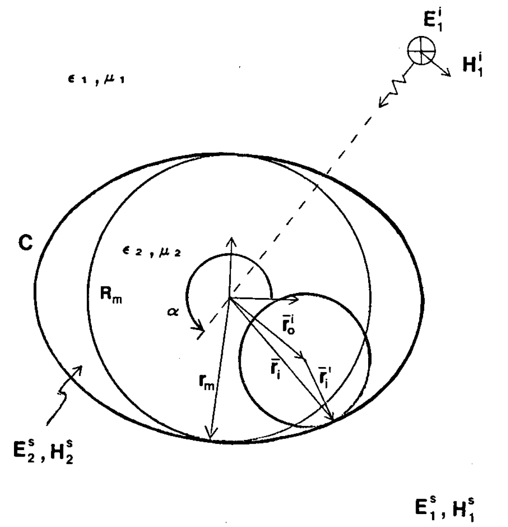

Fig. 2. Two-dimensional homogeneous dielectric elliptic cylinder.

sponding equivalent magnetic and electric currents along the contour C [8], [12].

IV. Scattering by a Convex Shaped Dielectric Cylinder

Motivated by the straightforward modal solution for the circular dielectric cylinder, the electromagnetic scattering and interaction by a convex homogeneous dielectric cylinder is discussed in the following. Based on the earlier discussion using (5b), the concept of the analytical continuation is invoked [10], [11] to treat noncircular convex geometries. The analytical continuation technique has been successfully applied previously for scattering by noncircular objects [10], but the formulation required rigorous treatment of the analytical field continuation for both the external region and also internal region of the dielectric scatterer. Instead, based on the OSRC relationship (3a), the analysis procedure discussed here requires analytical continuation only for the internal region, and provides an efficient technique for the case of noncircular convex homogeneous dielectric objects.

Let us consider the geometry of a homogeneous dielectric elliptic cylinder shown in Fig. 2. The excitation is assumed to be a TM polarized plane wave in region 1, and is normally incident on the dielectric scatterer. The analytic continuation procedure begins by determining the largest circle centered at the origin that can be completely contained inside the scatterer or on its contour C (denoted by the R_m circle). Inside this circle, we represent the electric field by the following primary modal expansion

$$E_2^s(r, \phi) = \sum_{n=-\infty}^{\infty} b_n j^{-n} J_n(k_2 r) e^{jn\phi} \tag{7}$$

where b_n are unknown coefficients. Since the expansion (7) is not convergent everywhere on the surface of the scatterer, it cannot be substituted directly into the expression (3a). Instead, we define a set of secondary field expansions each with a circle of convergence (denoted as R_0^i circle) completely contained in the object, and on its boundary a point on contour C. If the boundary C is discretized into W points with coordinates defined by $\bar{r}_i$, where $i = 1, 2, 3, \cdots, W$, then W of these secondary expansions are applied to the OSRC relationship (3a) at these specific points. The origin for the ith secondary expansion is chosen to be the point $\bar{r}_0^i$ which will be chosen to contain inside the R_m circle. It is noted here that for an elongated scattering object, it is not always possible to find a point $\bar{r}_0^i$ satisfying the above criteria. A solution to this case will be discussed briefly later based on the use of additional analytic continuations [10]. A secondary modal expansion is now defined to represent the axial electric field inside the R_0^i circle

$$E_2^s(r', \phi') = \sum_{m=-\infty}^{\infty} b'_m j^{-m} J_m(k_2 r') e^{jm\phi'}. \tag{8}$$

Since this expansion is valid at the boundary point $\bar{r}_i$, it can be used in the OSRC relationship (3a) at $\bar{r}_i$. The secondary field expansion (8) can now be related to the primary field expansion (7) using the analytic continuation theorem [9]–[11] which states that if the center of the circle of convergence of one expansion is contained inside the circle of convergence of another expansion, then in the region of overlap of the two circles of convergence, the two field expansions can be equated. Hence, the field expansions (7) and (8) are equal in some region of overlap in the interior of the dielectric scattering object. The exact location of this region is not important—only the fact that it exists. Thus

$$\sum_{n=-\infty}^{\infty} b_n j^{-n} J_n(k_2 r) e^{jn\phi} = \sum_{m=-\infty}^{\infty} b'_m j^{-m} J_m(k_2 r') e^{jm\phi'}. \tag{9a}$$

The addition theorem [13] for Bessel functions of the first kind gives

$$J_n(k_2 r) e^{jn\phi} = \sum_{m=-\infty}^{\infty} J_{n-m}(k_2 r_0^i) e^{j(n-m)\phi_0^i} J_m(k_2 r') e^{jm\phi'}. \tag{9b}$$

Substitution of the expression (9b) into (9a) yields

$$b'_m = \sum_{n=-\infty}^{\infty} b_n j^{n-m} J_{m-n}(k_2 r_0^i) e^{j(n-m)\phi_0^i}. \tag{9c}$$

The expression (9c) relates the unknown coefficients of the ith secondary expansion to the unknown coefficients of the primary expansion, and thus, allows one to relate each secondary expansion to the primary field expansion. In practical applications where the electrical size of the object will be known, the infinite summation in the above expansions can be conveniently truncated. The discussion on the truncation indices is provided later in this section. Truncating the secondary expansion (8) to some maximum index range $-M$ to M, and substituting it into (3a), an equation is obtained in the set of b_m. Similarly, truncating the series (9c) to some range $-N$ to N, and using it in this resulting equation, yields the following set of linear equations:

$$\sum_{m=-M}^{M} \sum_{n=-N}^{N} b_n j^{n-m} J_{m-n}(k_2 r_0^i) e^{j(n-m)\phi_0^i} B_2^+ \cdot \left[j^{-m} J_m(k_2 r') e^{jm\phi'} \right] = B_2 E_1^i(\bar{r}), \quad \text{for } \bar{r} = \bar{r}_i, \bar{r}' = \bar{r}_i'. \tag{10}$$

It is noted that the differentiation in the B_2 and B_2^+ operators is with respect to the unprimed coordinate system, while the expansion (10) is a function of the primed coordinates, so that care is taken to include the coordinate transformation when determining the required derivatives. The expression (10) is repeated for all the secondary expansions yielding a system of W linear equations, where W is the number of contour sampling points. Selecting W to be equal to $2N + 1$, where N is the primary series truncation index, results in a completely determined set of linear equations for the primary expansion coefficients b_n. Hence the following matrix equation is obtained

$$\bar{\bar{L}}\bar{B} = \bar{F} \tag{11a}$$

where

$$B_i = b_n \tag{11b}$$

$$F_i = B_2 E_1^i(\bar{r}) \,|_{\bar{r}=\bar{r}_i} \tag{11c}$$

$$L_{in} = \sum_{m=-M}^{M} j^{n-m} J_{m-n}(k_2 r_0^i) e^{j(n-m)\phi_0^i} B_2^+ \cdot \left[j^{-m} J_m(k_2 r') e^{jm\phi'} \right] |_{\bar{r}'=\bar{r}_i'} . \tag{11d}$$

Once the unknown primary expansion coefficients have been determined, the expression (9c) can be utilized to obtain the secondary expansion coefficients for each $\bar{r}_0^i$. This gives the required axial electric field at each contour point $\bar{r}_i$ as

$$E_2^s(\bar{r}_i) = \sum_{m=-M}^{M} \sum_{n=-N}^{N} b_n j^{n-m} J_{m-n}(k_2 r_0^i) e^{j(n-m)\phi_0^i} \cdot \left[j^{-m} J_m(k_2 r_i') e^{jm\phi_i'} \right]. \tag{12}$$

As mentioned earlier, the electric field on C obtained in (12) represents the magnetic surface current, and the normal derivative of the electric field on C represents the corresponding electric surface current distribution. Once the complete field distributions are known at the boundary contour C, the interior and the exterior field distributions including the far field distributions can be easily calculated [1], [8].

Returning to the question of truncation indices, in order to determine the index at which truncation of a field expansion is permissible, the electrical size of the region of validity of the series expansion is examined. For a given argument, the Bessel functions of the first kind of integer order decrease approximately for orders greater than the argument. Hence, the Bessel functions in field expansions (7) and (8) become negligible for orders greater than their maximum possible argument. Since the primary field expansion (7) is valid inside the R_m circle, its truncation index is given by

$$N \simeq k_2 r_m \tag{13a}$$

where r_m is the radius of the R_m circle. Similarly, the secondary field expansion (8) is valid only inside the circle centered at $\bar{r}_0^i$, so that its truncation index is given by

$$M \simeq k_2 |\bar{r}_i' - \bar{r}_0^i| . \tag{13b}$$

The limits stated in (13a) and (13b) are the minimum required, somewhat larger truncation indices than those above are selected.

It has been mentioned previously that it is not always possible to determine a suitable point $\bar{r}_0^i$ for every contour sampling point $\bar{r}_i$. This difficulty can be skirted by making successive continuations of the interior fields. Since the objective of the analytic continuation procedure is to obtain an inside scattered field expansion valid on the contour and related to the primary expansion, one can simply use more than one secondary field expansion to get from the R_m circle to the specific contour point of interest as discussed in [9]. For such objects, the analysis follows in an analogous fashion, and a similar matrix equation (11a) is obtained with the corresponding modified coefficient matrix elements given by

$$L_{in} = \sum_{p=-P}^{P} \sum_{m=-M}^{M} j^{n-m} J_{m-n}(k_2 r_0^i) e^{j(n-m)\phi_0^i} \cdot \left\{ j^{m-p} J_{p-m}(k_2 r'^i_0) e^{j(n-m)\phi'^i_0} \right\} \cdot B_2^+ \left[j^{-p} J_p(k_2 r'') e^{jm\phi''} \right] |_{\bar{r}'=\bar{r}_i'} . \tag{14}$$

The elaborate analysis details including discussion on the evaluation of matrix elements can be found in [9]. Still more elongated objects will require more than one of these auxiliary continuations, so that the matrix element expression for such objects will contain additional summations.

V. Numerical Results

Based on the analysis discussed above for the electromagnetic scattering and interaction by homogeneous convex dielectric objects, numerical results and their validations for the surface electric current and magnetic current distributions are presented for the case of a circular dielectric cylinder and an elliptic dielectric cylinder.

A. Homogeneous Circular Dielectric Cylinder

Fig. 3(a) show the magnitude and phase distribution of the surface electric current on a homogeneous circular dielectric cylinder based on both the OSRC formulation and the 'exact' eigenfunction series solution. These results are obtained by calculating the modal coefficients of (6), and then substituting the modal coefficients into the interior field expression 5(b). The dielectric cylinder has a relative permittivity of $\epsilon_r = 2$ and a relative permeability of $\mu_r = 2$. The radius of the circular cylinder is $a = 2.5$, and the frequency of excitation of the incident plane wave is such that the free space propagation constant $k_0 = 1$. Since the surface electric current distribution is symmetrical with respect to the direction of excitation, only the distribution for the range $\phi = 0$ to 180 is shown in the Fig. 3(a). For the same circular dielectric cylinder, Fig. 3(b) shows the magnitude and phase distribution of the surface magnetic currents. The OSRC results

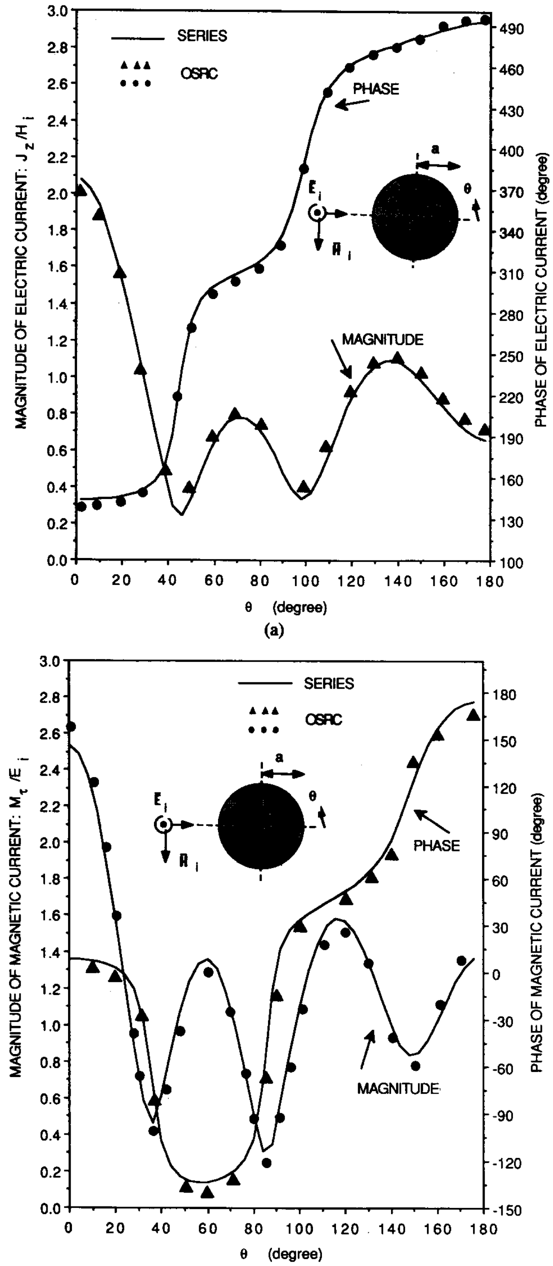

Fig. 3. (a) Magnitude and phase of electric current for dielectric circular cylinder ($k_0 = 1$, $a = 2.5$, $\epsilon = 2\epsilon_0$, $\mu = 2\mu_0$). (b) Magnitude and phase of magnetic current for dielectric circular cylinder ($k_0 = 1$, $a = 2.5$, $\epsilon = 2\epsilon_0$, $\mu = 2\mu_0$).

show good correspondence with the "exact" eigenfunction series solution.

B. Homogeneous Elliptic Dielectric Cylinder

The OSRC numerical result for the elliptic dielectric cylinder is obtained by solving the matrix equation (11a) for the various modal coefficients of (11b), and then the modal coefficients are substituted into the interior field expression (12). To effect such a solution, the coefficient matrix elements of (11d) are determined first. This involves applying the B_2^+ operator to the mth eigenfunction. Denoting these eigenfunctions as G in the unprimed rectangular coordinate system, and F in the primed cylindrical coordinate system, we have

$$G(x, y) = F(r', \phi') = \left[j^{-m} J_m(k_2 r') e^{jm\phi'}\right] \quad (15a)$$

$$r' = \left[(x - x_0)^2 + (y - y_0)^2\right]^{1/2} \quad (15b)$$

$$\phi' = \tan^{-1}\left(\frac{y - y_0}{x - x_0}\right). \quad (15c)$$

In order to consider arbitrary cross sections, if X and Y are the x and y components, respectively, of the normal vector on the elliptic scatterer, then the normal and second tangential derivatives contained in the B_2^+ operator can be calculated from

$$\frac{\partial}{\partial \nu} = X\frac{\partial}{\partial x} + Y\frac{\partial}{\partial y} \quad (16a)$$

$$\frac{\partial^2}{\partial s^2} = \left\{\frac{dx}{ds}\right\}^2 \left[\frac{\partial^2}{\partial x^2} + 2\frac{dy}{dx}\frac{\partial^2}{\partial x \partial y} + \left\{\frac{dy}{dx}\right\}^2 \frac{\partial^2}{\partial y^2} + \frac{d^2 y}{dx^2}\frac{\partial}{\partial y}\right] + \frac{d^2 x}{ds^2}\left[\frac{\partial}{\partial x} + \frac{dy}{dx}\frac{\partial}{\partial y}\right]. \quad (16b)$$

To calculate the derivatives given by (16a) and (16b), all the first- and second-order derivatives of G with respect to x and y are calculated using the chain rule and the coordinate transformation equations (15b) and (15c). The resulting expressions are then substituted into the B_2^+ operator and the matrix element expression (11d). After inclusion of the terms dependent on the scatterer geometry, the coefficient matrix is then completely specified. The general equations derived above can be specialized to the case of the elliptic dielectric cylinder [9].

Fig. 4(a) shows the magnitude and phase distribution of the surface electric current on a homogeneous dielectric cylinder based on the OSRC formulation. The elliptic dielectric cylinder has a relative permittivity of $\epsilon_r = 2$ and a relative permeability of $\mu_r = 1$. The semimajor axis of the elliptic cylinder is $k_0 a = 1$, and the semiminor axis is $k_0 b = 0.52$. The frequency of excitation of the incident plane wave is such that the free space propagation constant $k_0 = 2\pi$. Since the surface electric current distribution is symmetrical with respect to the direction of excitation as shown in the figure, only the distribution for the range $\phi = 90$ to 270 is shown in the Fig. 4(a). The OSRC results for the surface electric current distribution is compared with respect to the "exact" solution obtained based on the coupled combined field integral equation and method of moments technique [8]. For the same elliptic dielectric cylinder, Fig. 4(b) shows the magnitude and phase distribution of the surface magnetic currents. These results show good correspondence to the combined field integral equation solution. Once the surface electric and magnetic currents are known, the far-field distribution can be easily calculated [8], [9].

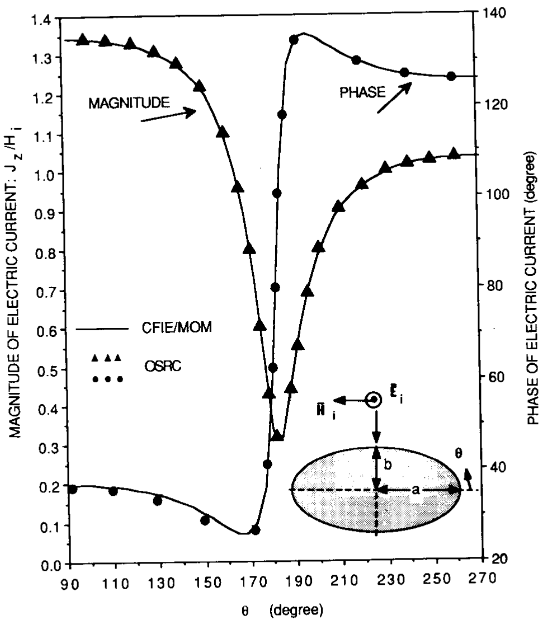

(a)

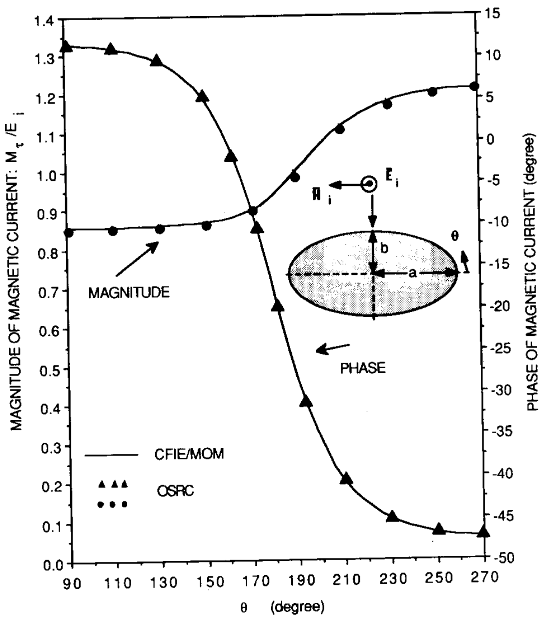

(b)

Fig. 4. (a) Magnitude and phase of electric current for dielectric elliptic cylinder ($k_0 = 2\pi$, $a = 1/2\pi$, $b = 0.52/2\pi$, $\epsilon = 2\epsilon_0$, $\mu = \mu_0$). (b) Magnitude and phase of magnetic current for dielectric elliptic cylinder ($k_0 = 2\pi$, $a = 1/2\pi$, $b = 0.52/2\pi$, $\epsilon = 2\epsilon_0$, $\mu = \mu_0$).

VI. Conclusion

The recent new analytical formulation of electromagnetic wave scattering by perfectly conducting two dimensional objects using the on-surface radiation boundary condition approach is successfully extended and validated for the case of two dimensional homogeneous convex dielectric objects. The classical scattering and penetration study of dielectric object is generally based upon the coupled field formulation with the external and internal fields directly coupled together. However, it is shown here that substantial simplification in the analysis can be obtained by applying the out-going radiation boundary condition directly on the surface of the convex homogeneous dielectric object. This approach decouples the fields in the two regions to yield explicitly a differential equation relationship between the external incident field excitation and the corresponding field distribution in the interior of the dielectric object. The interior fields are obtained by first solving the differential equation, using either an analytical approach or using a suitable numerical method. This technique can also be applied to conducting geometries with reentrant features and will be reported separately. Two-dimensional scattering examples along with validations are reported showing the near surface field distributions for a homogeneous circular dielectric cylinder and an elliptic dielectric cylinder with transverse magnetic plane wave excitation. The formulation and the corresponding results for the transverse electric polarization can be obtained based on the electromagnetic duality principle and are not reported here. The resulting surface electric and magnetic currents are compared and found in good agreement to those obtained from the coupled combined field integral equation solution.

References

[1] G. A. Kriegsmann, A. Taflove, and K. Umashankar, "A new formulation of electromagnetic wave scattering using an on-surface radiation boundary condition," *IEEE Trans. Antennas and Propagat.*, vol. AP-35, pp. 153-161, Feb. 1987.

[2] G. A. Kriegsmann and C. Morawetz, "Solving the Helmholtz equation for exterior problems with variable index of refraction: I," *SIAM J. Sci. Stat. Comput.*, vol. 1, pp. 371-385, Sept. 1980.

[3] A. Bayliss and E. Turkel, "Radiation boundary conditions for wave-like equations," *Commun. Pure Appl. Math.*, vol. 33, pp. 707-725, 1980.

[4] G. A. Kriegsmann and T. G. Moore, "An application of the on-surface radiation condition to the scattering of acoustic waves by a reactively loaded sphere," *Wave Motion*, vol. 10, pp. 277-284, 1988.

[5] G. Mur, "Absorbing boundary conditions for the finite-difference approximation of the time-domain electromagnetic field equations," *IEEE Trans. Electromagn. Compat.*, vol. EMC-23, pp. 377-382, Nov. 1981.

[6] L. N. Trefethen and L. Halpern, "Well-posedness of one-wave wave equations and absorbing boundary conditions," Inst. Comput. Appl. Sci. and Eng., NASA Langley Res. Cen., Hampton, VA, Rep. 85-30, June 1985.

[7] K. Umashankar and A. Taflove, "A novel method to analyze electromagnetic scattering of complex objects," *IEEE Trans. Electromagn. Compat.*, vol. EMC-24, pp. 397-405, Nov. 1982.

[8] —, "Analytical models for electromagnetic scattering," RADC/Hanscom AFB, MA, Final Tech. Rep. F19628-82-C-0140, June 1984.

[9] S. Arendt, "Application of the on-surface radiation condition method to two-dimensional electromagnetic scattering problems," M.S. thesis, Univ. Illinois, Chicago, IL, Apr. 1988.

[10] D. Wilton and R. Mittra, "A new numerical approach to the calculation of electromagnetic scattering properties of two-dimensional bodies of arbitrary cross section," *IEEE Trans. Antennas Propagat.*, vol. AP-20, pp. 310-317, May 1972.

[11] C. R. Mullin, R. Sandburg, and C. O. Velline, "A numerical technique for the determination of scattering cross sections of infinite cylinders of arbitrary geometrical cross section," *IEEE Trans. Antennas Propagat.*, vol. AP-13, pp. 141-149, 1965.

[12] A. J. Poggio and E. K. Miller, "Integral equation solutions of three dimensional problems," in *Computer Techniques for Electromagnetics*, R. Mittra, Ed. London: Pergamon, 1963, ch. 4.

[13] G. N. Watson, *A Treatise on the Theory of Bessel Functions*. Cambridge, MA: The University Press, 1966.

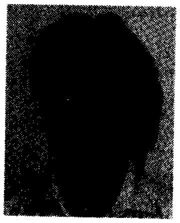

Stephen Arendt (S'85) received the B.S. and M.S. degrees in electrical engineering from the University of Illinois, Chicago, IL, in 1986 and 1988, respectively. He is currently pursuing the Ph.D. degree in physics at the University of Chicago, Chicago, IL.

Mr. Arendt is a member of Tau Beta Pi and Eta Kappa Nu.

Korada R. Umashankar (S'69–M'75–SM'81), for a photograph and biography please see pages 765 and 766 of the June 1986 issue of this TRANSACTIONS.

Allen Taflove (S'75–SM'84–F'90), for a photograph and biography please see page 1812 of the December 1988 issue of this TRANSACTIONS.

Gregory A. Kriegsmann, for a photograph and biography please see page 161 of the February 1987 issue of this TRANSACTIONS.